

Single-Well Monitoring of Protein–Protein Interaction and Phosphorylation–Dephosphorylation Events[†]

Mathieu Arcand,* Philippe Roby, Roger Bossé, Francesco Lipari, Jaime Padrós, Lucille Beaudet, Alexandre Marcil, and Sophie Dahan

PerkinElmer BioSignal Inc., 1744 William Street, suite 600, Montréal, Québec, Canada H3J 1R4

Received February 18, 2010; Revised Manuscript Received March 15, 2010

ABSTRACT: We combined oxygen channeling assays with two distinct chemiluminescent beads to detect simultaneously protein phosphorylation and interaction events that are usually monitored separately. This novel method was tested in the ERK1/2 MAP kinase pathway. It was first used to directly monitor dissociation of MAP kinase ERK2 from MEK1 upon phosphorylation and to evaluate MAP kinase phosphatase (MKP) selectivity and mechanism of action. In addition, MEK1 and ERK2 were probed with an ATP competitor and an allosteric MEK1 inhibitor, which generated distinct phosphorylation–interaction patterns. Simultaneous monitoring of protein–protein interactions and substrate phosphorylation can provide significant mechanistic insight into enzyme activity and small molecule action.

Throughout biology, protein structure and function are affected by post-translational modifications (PTMs) and interactions with diverse partners. Specifically, phosphorylation and protein–protein interaction (PPI) events ensure tight regulation and specific outputs in signal transduction (1). For phosphorylation and PPIs, multiplexing can be used to detect similar biomolecular events such as numerous phosphorylated molecules (2) or multiple interacting partners (3). Although the roles of protein phosphorylation and interaction are well-established in regulating signaling events, their interdependence, though often correlated, has not yet been directly measured.

Luminescent oxygen channelling (commercialized under the AlphaScreen and AlphaLISA trademarks) is an assay technology in which a biomolecule bridges a Donor and an Acceptor bead in proximity of each other. Laser excitation of the assay mixture elicits the formation of singlet oxygen which can migrate 200 nm from the Donor bead before reverting to its nonexcited state (4). When an Acceptor bead is within this 200 nm range, singlet oxygen molecules react with the dyes it bears to trigger light emission. In contrast to time-resolved fluorescence resonance energy transfer, this technology does not require specific spatial alignment of fluorescent molecules but relies rather on the long-range diffusion of singlet oxygen, which confers great flexibility in assay design. AlphaScreen and AlphaLISA technologies have namely been used to detect PPIs (5–7) as well as phosphorylation events (8, 9). AlphaScreen and AlphaLISA Acceptor beads contain different dyes that grant them distinct emission spectra (Figure 1a of the Supporting Information). AlphaScreen beads

harbor rubrene which emits broadly in the wavelength range of 560–620 nm and has an emission peak around 560 nm, while AlphaLISA beads are dyed with a europium chelate with a sharp emission peak at 615 nm. We have taken advantage of these different light emission properties to monitor substrate phosphorylation and PPIs in a single well. We used ERK2 as a model because this essential MAP kinase is tightly regulated by the phosphorylation of the threonine and tyrosine residues in its activation loop, as well as by docking interactions with upstream kinases such as MEK1, downstream effectors, scaffolding proteins, and negative regulators such as MKPs (10).

To set up assay conditions for the dual detection of phosphorylation and PPI, we first optimized detection of the two biomolecular events separately. We assayed PPIs using GSH Donor and nickel chelate AlphaLISA Acceptor beads. Hence, active histidine-tagged MEK1 (His-MEK1) was incubated with increasing concentrations of glutathione *S*-transferase-tagged unphosphorylated ERK2 [GST-ERK2 (Figure 1c of the Supporting Information)]. Complexed MEK1 and ERK2 proteins bridged GSH-coated Donor and nickel chelate-coated AlphaLISA Acceptor beads to allow signal generation and thus binding detection (Figure 1b of the Supporting Information). Maximal interaction was observed with His-MEK1 and GST-ERK2, each at an assay concentration of 100 nM, whereas no signal could be detected in absence of either counterpart.

We then monitored ERK2 phosphorylation by MEK1 in a complementary experimental configuration using a mouse monoclonal antibody recognizing the dual-phosphorylated activation loop threonine and tyrosine residues, in combination with anti-mouse antibody-conjugated AlphaScreen Acceptor beads. The assay setup was also completed by GSH-coated Donor beads binding to GST-ERK2 (Figure 1d of the Supporting Information). In this assay, GST-ERK2 was phosphorylated by active His-MEK1 in the presence of 10 μ M ATP. As expected, the magnitude of the signal was proportional to ERK2 and MEK1 concentrations in the assay, and maximal counts were observed with each partner at 100 nM (Figure 1e of the Supporting Information). Notably, no signal was generated in the absence of MEK1, thus indicating that unactive ERK2 does not autophosphorylate under these experimental conditions.

These individual tests with AlphaLISA and AlphaScreen beads indicated that both the binding and phosphorylation assays are optimal with 100 nM His-MEK1 and GST-ERK2. Since these two assays rely on GSH-coated Donor beads, we hypothesized that their merger could allow the simultaneous measurement of ERK2 phosphorylation by MEK1 and interaction between the two proteins (Figure 1a). To correlate appropriately these two distinct biomolecular events, active His-MEK1 and unphosphorylated

[†]M.A. is a recipient of the IRDF from the Natural Sciences and Engineering Research Council of Canada.

*To whom correspondence should be addressed. Phone: (514) 937-1010. Fax: (514) 937-0777. E-mail: mathieu.arcand@perkinelmer.com.

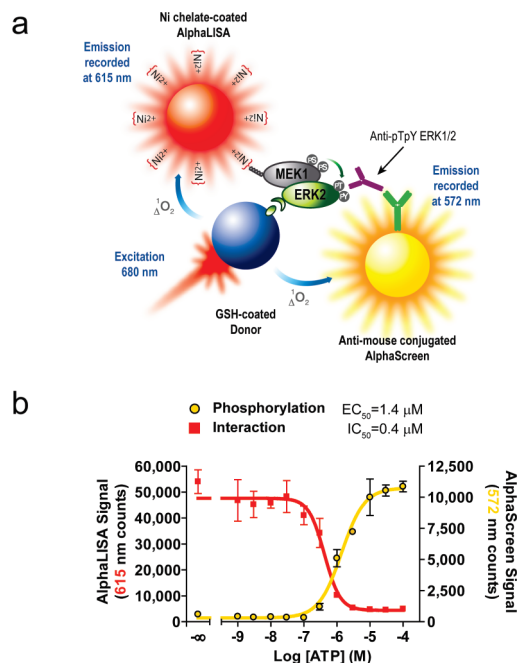


FIGURE 1: ERK2 dissociation upon phosphorylation by MEK1. (a) Dual-assay configuration obtained by combined use of Ni-coated AlphaLISA Acceptor beads to monitor His-MEK1 and GST-ERK2 binding and AlphaScreen-coupled phosphorylation detection. Narrow bandwidth filters were used for sequential reading of the AlphaScreen signal followed by the AlphaLISA signal. (b) Phosphorylated His-MEK1 was incubated with the unphosphorylated GST-ERK2 protein in the presence of increasing concentrations of ATP. Phosphorylation and interaction events were simultaneously monitored as depicted in panel a [(red squares) AlphaLISA 615 nm signal with MEK1–ERK2 interaction and (gold circles) AlphaScreen 572 nm signal with ERK2 phosphorylation].

GST-ERK2 were co-incubated in an equimolar ratio in the presence of increasing ATP concentrations (Figure 1b). The simultaneous monitoring of phosphorylation and interaction events was achieved using narrow bandwidth filtering of the AlphaScreen and AlphaLISA light emission signals, respectively. This assay revealed a close correlation between ERK2 activation loop dual phosphorylation and its dissociation from MEK1 (see the Supporting Information for further discussion). To the best of our knowledge, this represents the first direct detection in a single experiment of a dynamic phenomenon encompassing these two distinct biomolecular events.

To ensure signal specificity and assay robustness, assays were repeated via substitution of the anti-mouse conjugated AlphaScreen or nickel chelate-coated AlphaLISA beads with their respective unconjugated counterparts, or by withdrawing the phosphorylation-specific antibody (Figure 2a of the Supporting Information). As expected, withdrawal of essential assay components resulted in the loss of the corresponding signal without affecting the other. Additionally, control experiments using swapped AlphaScreen and AlphaLISA beads (Figure 2b of the Supporting Information) confirmed the specificity of the detection method. Importantly, we observed that the best signal-to-background ratios in a dual-assay configuration were obtained with AlphaScreen beads for monitoring phosphorylation and with AlphaLISA beads for monitoring interaction.

After demonstrating the inverse relationship between phosphorylation and interaction occurring in a kinase cascade, we sought to monitor dephosphorylation reactions. Dual-specificity MAP kinase phosphatases catalyze the deactivation of MAP

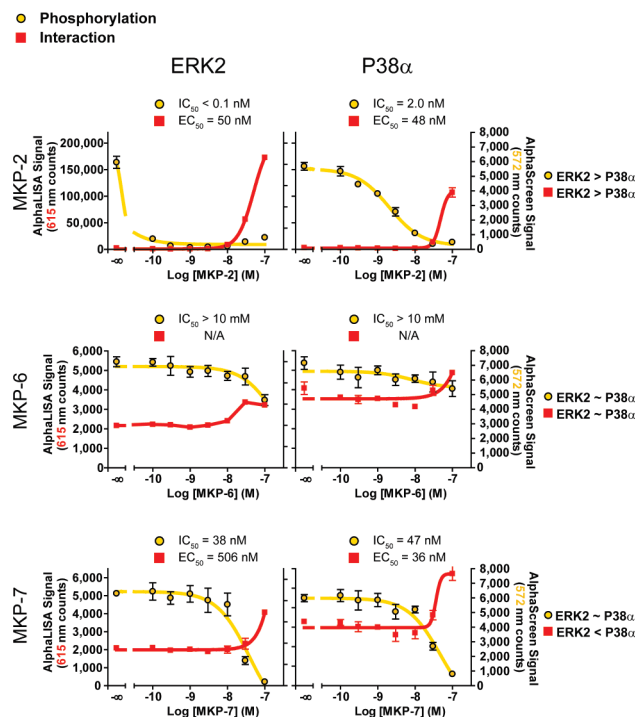


FIGURE 2: Selectivity mechanism for three MAP kinase phosphatases. MKP-2, MKP-6, and MKP-7 exhibit different mechanisms of action. Each MKP acts similarly on ERK2 and P38α but exhibits different selectivities in terms of catalytic activity [(gold circles) AlphaScreen 572 nm signal with ERK2 or P38α dual phosphorylation] and PPI [(red squares) AlphaLISA 615 nm signal with MKP–MAP kinase interaction].

kinases by dephosphorylating both of their activating residues (11). MKPs display diverse subcellular localizations and substrate selectivity. In addition, some harbor MAP kinase docking motifs that confer upon them interaction selectivity (Figure 3a of the Supporting Information). Despite their established role as negative MAP kinase regulators, MKPs' mechanisms of action remain incompletely characterized, and their selectivity is still elusive. We used the dual phosphorylation–interaction assay to determine the selectivity of three His-tagged MKPs toward ERK2 and P38α MAP kinases, as well as to obtain mechanistic insight into their action (Figure 3b of the Supporting Information). On both substrates, the order of potency for dephosphorylation was as follows: MKP-2 \gg MKP-7 > MKP-6 (based on IC₅₀ values). Moreover, MKP-2 displayed more potency for dephosphorylation of ERK2 versus P38α (Figure 2, top panels). At equimolar concentrations, MKP-2 significantly interacted with the dephosphorylated forms of P38α and ERK2, interaction with the latter yielding a stronger signal. This is in agreement with reported data which show that ERK2 exhibits better MKP-2 binding and significantly enhances MKP-2 phosphatase activity, in comparison to P38α (12). Distinguishably, MKP-6 exhibited significantly less activity and binding toward ERK2 and P38α, with both substrates being only partially dephosphorylated at a MKP-6 concentration of 100 nM (Figure 2, middle panels). MKP-7 exerted similar dephosphorylation activity toward ERK2 and P38α but interacted preferably with P38α (Figure 2, bottom panels). Taken together, these results demonstrate that MKP-2, MKP-6, and MKP-7 exhibit different mechanisms of action and selectivity.

A dual assay for the simultaneous monitoring of protein binding and phosphorylation may enable detailed assessment

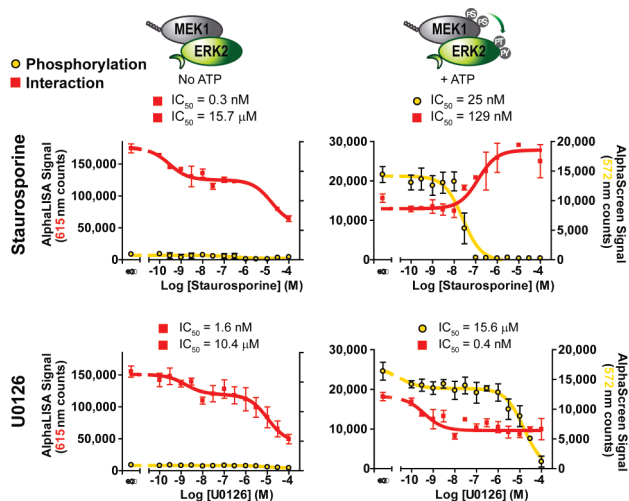


FIGURE 3: Different inhibition patterns from an ATP competitor and an allosteric modulator. Unactive GST-ERK2 was incubated with unactive His-MEK1 (left) or active His-MEK1 and 10 μM ATP (right) and with increasing concentrations of the generic kinase inhibitor staurosporine (top) or with the MEK1/2 allosteric inhibitor U0126 (bottom). Phosphorylation and interaction events were simultaneously monitored as depicted in Figure 1a [(gold circles) AlphaScreen 572 nm signal with ERK2 phosphorylation and (red squares) AlphaLISA 615 nm signal with MEK1–ERK2 PPIs]. Staurosporine and U0126 each display a two-site inhibition effect on inactive MEK1 and ERK2 interaction, and IC₅₀ values reported refer solely to interaction (left). In contrast, when phosphorylation could occur, phosphorylation and interaction IC₅₀ values are reported (right).

of pharmacological inhibitors' mechanisms of action by discriminating between ATP competitors and allosteric modulators. Two inhibitors, namely, staurosporine and U0126, were thus tested for their ability to modulate both the phosphorylation and interaction events between MEK1 and ERK2, either as unactive binding partners (Figure 3, left panels) or with active MEK1 acting on unphosphorylated ERK2 in the presence of ATP (Figure 3, right panels). Staurosporine is a highly promiscuous pan-kinase inhibitor that mimics ATP and acts as a competitor for the binding to the kinase catalytic cleft (13). As expected, staurosporine completely inhibited ERK2 phosphorylation by MEK1, which in turn partially restored their interaction (Figure 3, top right panel). Interestingly, in the absence of ATP, staurosporine affected unactive MEK1 and ERK2 in a biphasic manner (Figure 3, top left panel), consistent with the binding of the compound to both kinases with affinities differing by several orders of magnitude, as reported previously (13). In sharp contrast to staurosporine, U0126, an allosteric and non-ATP competitive MEK1/2 inhibitor (14), also blocked ERK2 phosphorylation, but it did not restore PPI (Figure 3, bottom right panel). Moreover, U0126 disrupted the interaction between unactive MEK1 and ERK2 also in a biphasic manner (Figure 3, bottom left panel), consistent with the compound acting more strongly on MEK1 than ERK2 (15). These data indicate that phosphorylation–interaction patterns can provide important

mechanistic insights into the action of pharmacological inhibitors.

AlphaScreen and AlphaLISA technologies are widely used in compound screening campaigns, and one can easily foresee the applicability of our dual technology to identification of modulators of catalytic activity and/or PPI. Plotting simultaneous phosphorylation and interaction signals generates characteristic signature patterns. These patterns can in turn be used to compare the action of different enzymes on a substrate and to provide insights into the mechanism of action of small molecules. Furthermore, the versatility of this detection method makes it amenable for use outside of the phosphorylation field to monitor PTM and simultaneous PPIs.

SUPPORTING INFORMATION AVAILABLE

Experimental methods, supplementary table, figures, and discussion. This material is available free of charge via the Internet at <http://pubs.acs.org>.

REFERENCES

1. Ubersax, J. A., and et Ferrell, J. E. (2007) *Nat. Rev. Mol. Cell Biol.* 8, 530–541.
2. Du, J., Bernasconi, P., Clauser, K. R., Mani, D. R., Finn, S. P., Beroukhi, R., Burns, M., Julian, B., Peng, X. P., Hieronymus, H., Maglathlin, R. L., Lewis, T. A., Liao, L. M., Nghiemphu, P., Mellinghoff, I. K., Louis, D. N., Loda, M., Carr, S. A., Kung, A. L., and et Golub, T. R. (2009) *Nat. Biotechnol.* 27, 77–83.
3. Mayer, B. J. (2006) *Methods Mol. Biol.* 332, 79–99.
4. Ullman, E. F., Kirakossian, H., Singh, S., Wu, Z. P., Irvin, B. R., Pease, J. S., Switchenko, A. C., Irvine, J. D., Dafforn, A., and et Skold, C. N. (1994) *Proc. Natl. Acad. Sci. U.S.A.* 91, 5426–5430.
5. Stokka, A. J., Gesellchen, F., Carlson, C. R., Scott, J. D., Herberg, F. W., and et Taskén, K. (2006) *Biochem. J.* 400, 493–499.
6. Mohamed, M. R., Rahman, M. M., Lanchbury, J. S., Shattuck, D., Neff, C., Dufford, M., van Buuren, N., Fagan, K., Barry, M., Smith, S., Damon, I., and et McFadden, G. (2009) *Proc. Natl. Acad. Sci. U.S.A.* 106, 9045–9050.
7. Partch, C. L., Card, P. B., Amezcua, C. A., and et Gardner, K. H. (2009) *J. Biol. Chem.* 284, 15184–15192.
8. Von Leoprechting, A., Kumpf, R., Menzel, S., Reulle, D., Griebel, R., Valler, M. J., and et Büttner, F. H. (2004) *J. Biomol. Screening* 9, 719–725.
9. Guenat, S., Rouleau, N., Biemann, C., Bedard, J., Maurer, F., Allaman-Pillet, N., Nicod, P., Bielefeld-Sévigny, M., Beckmann, J. S., Bonny, C., Bossé, R., and et Roduit, R. (2006) *J. Biomol. Screening* 11, 1015–1026.
10. Raman, M., Chen, W., and et Cobb, M. H. (2007) *Oncogene* 26, 3100–3112.
11. Owens, D. M., and et Keyse, S. M. (2007) *Oncogene* 26, 3203–3213.
12. Chen, P., Hutter, D., Yang, X., Gorospe, M., Davis, R. J., and et Liu, Y. (2001) *J. Biol. Chem.* 276, 29440–29449.
13. Karaman, M. W., Herrgard, S., Treiber, D. K., Gallant, P., Atteridge, C. E., Campbell, B. T., Chan, K. W., Ciceri, P., Davis, M. I., Edeen, P. T., Faraoni, R., Floyd, M., Hunt, J. P., Lockhart, D. J., Milanov, Z. V., Morrison, M. J., Pallares, G., Patel, H. K., Pritchard, S., Wodicka, L. M., and et Zarrinkar, P. P. (2008) *Nat. Biotechnol.* 26, 127–132.
14. Davies, S. P., Reddy, H., Caivano, M., and et Cohen, P. (2000) *Biochem. J.* 351, 95–105.
15. Bain, J., Plater, L., Elliott, M., Shpiro, N., Hastie, C. J., McLauchlan, H., Klevornic, I., Arthur, J. S. C., Alessi, D. R., and et Cohen, P. (2007) *Biochem. J.* 408, 297–315.